

Thermal studies of some purine compounds and their metal complexes

M. S. Masoud · A. El-Merghany · A. M. Ramadan ·
M. Y. Abd El-Kaway

Received: 11 May 2009/Accepted: 10 February 2010/Published online: 28 March 2010
© Akadémiai Kiadó, Budapest, Hungary 2010

Abstract The mechanism of the decomposition of the entitled compounds and their complexes is studied. Adenine, its Schiff base of salicylaldehyde, and its azo resorcinol derivatives are ended with carbon. However, oxalonitrile compound is appeared as a final product for adenine acetylacetone and an intermediate for adenine. The thermodynamic parameters of the decomposition reaction were evaluated and discussed. The change of entropy values, $\Delta S^\#$, showed that the transition states are more ordered than the reacting complexes. The thermal processes proceed in complicated mechanisms where the bond between the central metal ion and the ligands dissociates after losing small molecules such as H_2O , NH_3 , or HCl . In most cases, the free radical species of the ligands are assigned to exist through decomposition mechanisms. The copper adenine and nickel salicylaldehyde complexes are ended with the metal as a final product. However, the cobalt adenine, its acetylacetone, its salicylaldehyde, cadmium and mercury guanine complexes are ended with metal oxides.

Keywords Purines compounds · Arylazo derivatives · Metal complexes · Thermal analysis

Introduction

Compounds containing pyrimidine and purine play a significant role in many biological systems [1–3], where both exist in nucleic acids, several vitamins, coenzymes, and antibiotics. These provide potential binding sites for metal ions, and any information on their coordinating properties is important as a means of understanding the role of the metal ions in biological systems. Vitamin B4, also known as adenine, is one of the two purine bases used in forming nucleotides of the nucleic acids DNA and RNA. It acts as a co-enzyme with other substances, such as other vitamins to produce energy mostly from the mitochondria, which are the power producers of a cell. The food we eat is the fuel that is “burned” inside the mitochondria to produce energy where complex carbohydrates produce the best fuel contain Vitamin B-4. An “adenosine triphosphate” (ATP) consists of three substances: adenine, ribose, and three phosphate groups, and is also produced during “photosynthesis.” Adenine plays a vital role in red and white blood cell formation and considered to be a catalyst in helping to improve lactation for a nursing mother. The systematic study of metal ion-nucleic acid interactions has many roots. The realization that nucleic acids are strong acids, i.e., require cations, hence metal ions or protonated amines, was among the earliest. Cisplatin (*cis*-[Pt(NH₃)₂Cl₂]) being a potent anti-tumor agent [4] and subsequent work strongly suggesting that Pt-DNA binding was responsible for triggering tumor cell killing, proved a climax in the field. Owing to the role played by these complexes in many metabolic processes, their structure and stereochemistry are a matter of considerable interest [5, 6]. Attention in our laboratory has escalated regarding the potential of about the chemistry of nucleic acid constituents and their complexes [7–16]. Twenty three purine complexes [17] of iron, cobalt, nickel,

M. S. Masoud (✉) · A. M. Ramadan · M. Y. Abd El-Kaway
Department of Chemistry, Faculty of Science, Alexandria
University, Alexandria, Egypt
e-mail: drmsmasoud@yahoo.com

A. El-Merghany
Department of Chemistry, Faculty of Science, Suez-Canal
University, Suez, Egypt

copper, cadmium, mercury are mixed (Ni–Cr, Co–Cu). The ligands used are: adenine, guanine, adenine Schiff base of acetylacetone, adenine Schiff base of salicylaldehyde, adenine azo resorcinol. The analytical data of the complexes typified the formation of stoichiometries 1:1, 1:2, 1:3 (M:L). The complexes are with different geometries: square planar, tetrahedral, and octahedral. The mode of bonding was identified by IR spectra [17]. The thermal analysis is an important tool in studying the thermal stability and the kinetics of complexes [18–21]. In a sequel of continuation, the main interest of this article is studying the thermal behavior of some selected complexes of these purine compounds and their complexes. The mechanism of decomposition is explained, and the thermodynamic parameters are evaluated and discussed.

Experimental

Materials and methods

Ligands

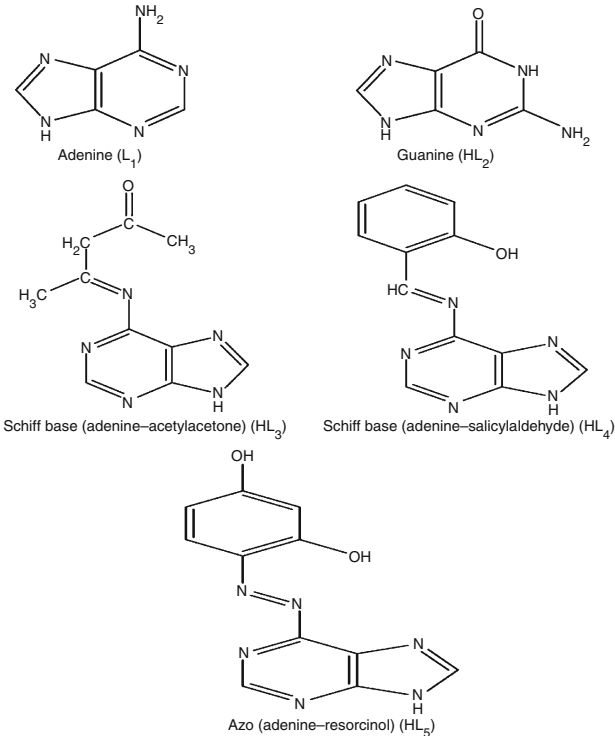
Adenine (L_1) with the molecular formula $C_5H_5N_5$ and molecular mass 135.13 was purchased from Riedel-de Haen Company. Guanine (HL_2) with the molecular formula $C_5H_5N_5O$ and molecular mass 151.13 was purchased from Fluka Company. Two selected Schiff base compounds were prepared of adenine (as an amine) with acetylacetone (HL_3) and salicylaldehyde (HL_4) as follows: 0.01 mol of adenine and a few amount of hot ethanol were added dropwise with continuous stirring to a hot ethanolic solution of 0.01 mol of acetylacetone and 0.01 mol of salicylaldehyde. The reaction mixture was refluxed on water bath for about 30 min with constant stirring and then allowed to cool at room temperature. The separated solid products were filtered off and cooled at room temperature and crystallized from ethanol. The azo adenine-resorcinol ligand (HL_5) was prepared by dissolving 0.1 mol of adenine in 0.2 mol HCl and 25 mL distilled water. The hydrochloride compound was diazotized below 5 °C with a solution of $NaNO_2$ (0.1 mol) and 20-mL distilled water. The diazonium chloride was coupled with an alkaline solution of 0.1 mol resorcinol/30-mL distilled water.

Complexes

All the complexes were prepared in a similar manner. The inorganic salts [Fe, Co, Ni, Cu, Cd, Hg as chlorides] and the ligands were dissolved in water and in ethanol–water media, respectively. Only copper azo adenine resorcinol complexes, $CuL_5(OH)$, was prepared in ammoniacal media. The complexes were prepared using different mole

ratio (M:L). Also, two mixed complexes were prepared: Ni–Cr–adenine and Co–Cu–guanine with the mole ratio 1:1:5 and 1:1:3, respectively. The ligands and their complexes were characterized by elemental analysis, magnetic measurements and spectral measurements [17] (Scheme 1).

Differential thermal (DTA) and thermogravimetric analysis (TG) were carried out using a Shimadzu DTA/TG-50. The rate of heating was 5 °C min⁻¹. The cell used was platinum, the atmospheric nitrogen was flowed over the sample at a rate 20 cm³ min⁻¹ and a chamber cooling



Scheme 1 The structure of the ligands

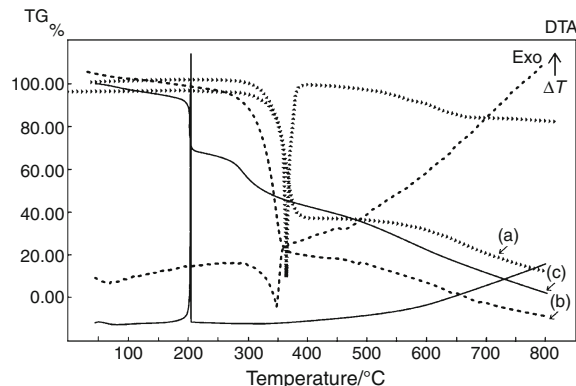


Fig. 1 TG and DTA curves of: **a** adenine (L_1), **b** adenine-acetylacetone (HL_3), and **c** azo adenine-resorcinol (HL_5)

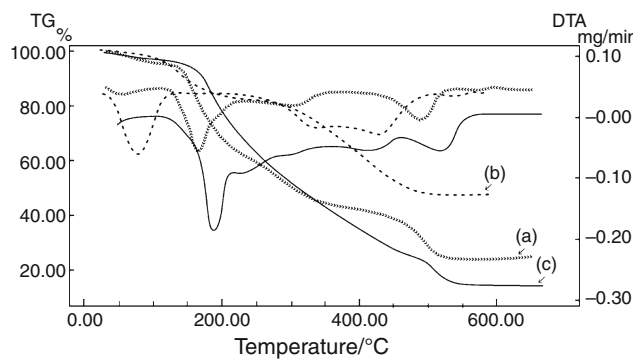


Fig. 2 TG and DTA curves of: **a** Co-adenine (L_1), **b** Hg-guanine (HL_2), and **c** Co-adenine-salicylaldehyde (HL_4)

water flow rate was $10 \text{ L}^{-1} \text{ h}^{-1}$. The instrument was located at the central laboratory, Faculty of Science, Cairo University. The DTA and TG thermograms of three ligands (L_1 , HL_3 , and HL_5 ; Fig. 1) and three complexes representing the ligands (L_1 , HL_2 , and HL_4 ; Fig. 2) are selected for demonstration. The DTA data of ligands and complexes are represented in Table 1.

Calculation

The order of chemical reactions (n) was calculated via the peak symmetry method by Kissinger [22]. The asymmetry of the peak, S , is calculated as follows:

Table 1 Thermodynamic parameters of the ligands and their complexes

Compound	Peak (type)	Slope (DTA)	$\Delta E/\text{kJ mol}^{-1}$	a	b	S (shape index)	n	α_m	T_m/K	Z/s^{-1}	$\Delta S/\text{kJ K}^{-1} \text{ mol}^{-1}$	$\Delta H/\text{kJ mol}^{-1}$
L_1	Endo	-13.75	114.31	1.3	2.9	0.45	0.8436	0.6629	636.52	1.117	-0.2503	-159.321
	Endo	-10.46	86.96	3.3	5.0	0.66	1.0236	0.6278	940.05	0.562	-0.2592	-243.696
HL_3	Endo	-9.027	75.05	3.5	5.8	0.60	0.9787	0.6360	619.84	0.745	-0.2534	-157.092
HL_4	Endo	-10.75	89.417	1.0	2.4	0.42	0.8133	0.6694	404.11	1.421	-0.2445	-98.8127
	Endo	-17.22	143.20	0.3	2.1	0.14	0.4762	0.7574	477.44	1.945	-0.2433	-116.159
HL_5	Exo	VERY	SHARP	PEAK								
	Endo	-16.25	135.16	0.7	2.0	0.35	0.7454	0.6846	524.11	1.645	-0.2454	-128.65
	Endo	-18.39	152.91	3.4	1.6	2.12	1.8367	0.5164	568.55	1.712	-0.2458	-139.755
$\text{Co}\cdot(L_1\text{-H})\cdot\text{Cl}\cdot2\text{H}_2\text{O}$	Exo	VERY	SHARP	PEAK								
	Endo	-8.505	70.713	2.2	1.9	1.16	1.3558	0.5749	448.34	1.649	-0.2441	-109.46
$\text{Cu}\cdot2(L_1)\cdot2\text{Cl}$	Endo	-23.83	198.18	1.2	1.9	0.63	1.0013	0.6318	832.09	2.471	-0.2459	-204.633
	Endo	-9.12	75.842	2	1.1	1.80	1.6989	0.5315	343.00	1.436	-0.2430	-83.3712
$\text{Cd}\cdot(L_2)\cdot\text{Cl}\cdot\text{H}_2\text{O}$	Endo	-20.83	173.18	0.5	0.7	0.71	1.0648	0.6204	485.50	2.343	-0.2418	-117.436
	Exo	SHARP	PEAK									
	Endo	-36.53	303.73	1.3	0.5	2.60	2.0316	0.4969	548.00	3.764	-0.2389	-130.946
$\text{Hg}\cdot(HL_2)\cdot2\text{Cl}\cdot\text{H}_2\text{O}$	Endo	-9.69	80.613	1.9	2.8	0.67	1.0379	0.6252	650.50	0.762	-0.2536	-165.002
	Endo	-13.73	114.22	2.5	1.7	1.47	1.5279	0.552	446.91	2.744	-0.2398	-107.207
	Endo	-11.89	98.861	0.7	1.6	0.44	0.8334	0.6650	603.43	1.696	-0.2463	-148.673
$\text{Co}\cdot(HL_3)\cdot2\text{Cl}\cdot\text{H}_2\text{O}$	Endo	-25.75	214.13	1.7	2.9	0.59	0.9647	0.6387	742.56	3.028	-0.2432	-180.656
	Endo	-6.2.2	51.563	2	2.1	0.95	1.2296	0.5935	361.13	1.500	-0.2431	-87.8021
	Endo	-10.11	84.054	2.5	3.6	0.69	1.05	0.6231	818.76	1.044	-0.2529	-207.105
$\text{Co}\cdot(HL_4)\cdot2\text{Cl}\cdot4\text{H}_2\text{O}$	Endo	-25.08	208.58	1	1.2	0.83	1.1502	0.6060	447.60	5.294	-0.2344	-104.933
	Endo	-27.61	229.61	4.8	1.1	4.36	2.6320	0.4473	551.09	5.005	-0.2360	-120.62
	Endo	-30.07	250.05	1.7	1.9	0.89	1.1918	0.5994	755.53	3.497	-0.2422	-183.017
$\text{Ni}\cdot(HL_4)\cdot2\text{Cl}\cdot5\text{H}_2\text{O}$	Endo	-11.18	92.975	1	0.6	1.67	1.6266	0.5399	460.80	2.131	-0.2422	-111.624
	Endo	-22.48	186.90	1.5	1.1	1.36	1.4713	0.5592	509.58	4.008	-0.2378	-121.191
	Endo	-11.98	99.659	1.7	2.7	0.63	0.9998	0.6321	690.07	1.484	-0.2486	-171.556
	Endo	-19.87	165.23	1.6	2.5	0.64	1.008	0.6306	790.07	2.164	-0.2466	-194.83
$\text{Ni}\cdot(HL_4)\cdot2\text{Cl}\cdot5\text{H}_2\text{O}$	Endo	-5.016	41.707	2.8	1.1	2.54	2.0102	0.4990	328.38	1.334	-0.2433	-79.924
	Endo	SHARP	PEAK									
	Endo	-5.27	43.814	3.8	2.2	1.73	1.6559	0.5364	565.30	0.789	-0.2521	-142.566
	Endo	-10.98	91.31	1.7	4.6	0.37	0.7659	0.6799	863.76	1.075	-0.2531	-218.66

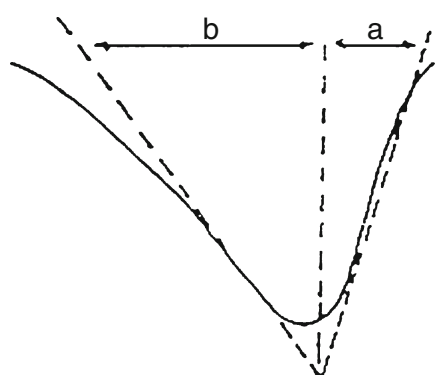


Fig. 3 The peak symmetry method

$$S = 0.63n^2$$

$$n = 1.26(a/b)^{1/2}.$$

(Fig. 3).

The value of the decomposed substance fraction, α_m , at the moment of maximum development of reaction (with $T = T_m$) being determined from the relation [23]:

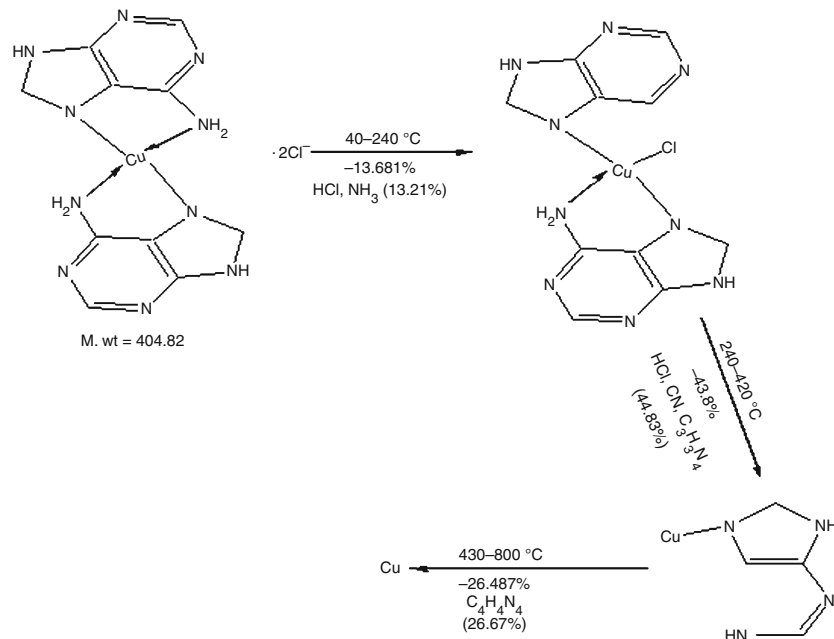
$$(1 - \alpha_m) = n^{1-n}.$$

The values of collision factor, Z , can be obtained in case of Horowitz Metzger by making the use of the relation [24]:

$$z = \frac{E}{RT_m} \phi \exp\left(\frac{E}{RT_m^2}\right) = \frac{KT_m}{h} \exp\left(\frac{\Delta S^\#}{R}\right),$$

where $\Delta S^\#$ is the entropies of activation, R represents molar gas constant, ϕ rate of heating ($K s^{-1}$), K the Boltzmann constant, and h the Planck's constant [25]. The change in

Scheme 2 The TG mass losses of the 1:2 copper adenine complex



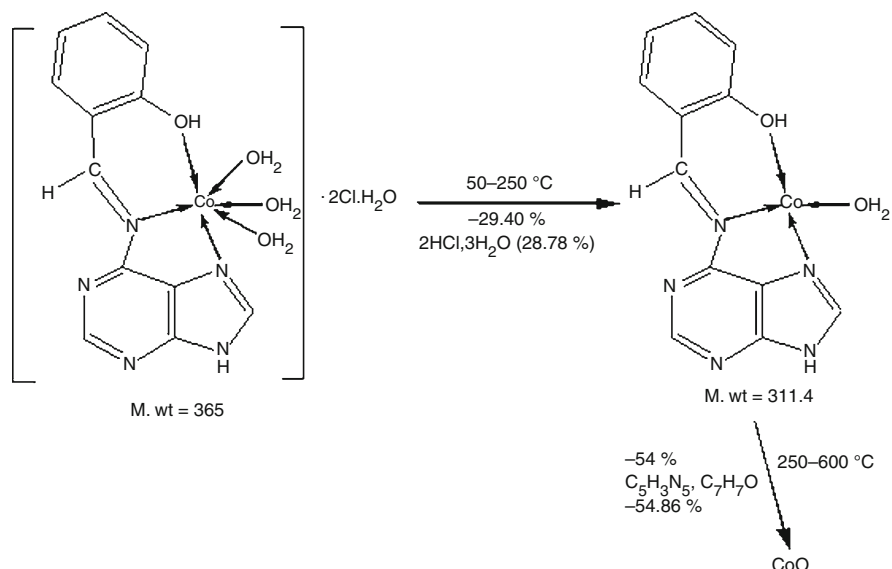
enthalpy ($\Delta H^\#$) for any phase transformation [26] taking place at any peak temperature, T_m , can be given by the following equation: $\Delta S^\# = \Delta H^\#/T_m$. Based on least square calculations, the $\ln \Delta T$ versus $1000/T$ plots for all complexes, for each DTA curve, gave straight lines from which the activation energies were calculated according to the methods of Piloyan et al. [27]. The slope is of Arrhenius type and equals to $-E/R$.

Results and discussion

The thermal properties are recorded for four ligands: adenine (L_1), Schiff base adenine-acetylacetone (HL_3), Schiff base adenine-salicylaldehyde (HL_4), and the azo adenine-resorcinol (HL_5). However, the thermal data are given for seven complexes: two of adenine: $Co \cdot (L_1 \cdot H) \cdot Cl \cdot 2H_2O$ and $Cu \cdot 2(L_1) \cdot 2Cl$; three derived from Schiff bases: $Co \cdot (HL_3) \cdot 2Cl \cdot H_2O$, $Co \cdot (HL_4) \cdot 2Cl \cdot 4H_2O$, and $Ni \cdot (HL_4) \cdot 2Cl \cdot 5H_2O$; and two guanine (HL_2) complexes: $Cd \cdot (L_2) \cdot Cl \cdot H_2O$ and $Hg \cdot (HL_2) \cdot 2Cl \cdot H_2O$. The DTA curves exhibit a series of thermal changes during the increase of temperature. Some trends and conclusions may be achieved as follows:

- (i) All the first peaks of the DTA curves are assigned to dehydration processes of the outer sphere or coordinated water molecules except that at 343 K for the unhydrated Cu-adenine complex, $Cu \cdot 2(L_1) \cdot 2Cl$, is probably due to dehydrative removal of adsorbed water. While the middle and latter peaks could be assigned to material decomposition processes that proceed in complicated mechanisms where the bond between the central metal ion and the ligands dissociates after losing of small

Scheme 3 The TG mass losses of Co complex derived from adenine-salicylaldehyde (HL_4)



molecules such as H_2O , NH_3 , or HCl . The cobalt adenine, its acetylacetone, its salicylaldehyde, cadmium and mercury guanine complexes are ended with metal oxides [28]. However, the copper adenine and nickel adenine–salicylaldehyde complexes are ended with the metal as a final product. The TG mass losses of the 1:2 copper adenine complex suggested the following mechanism (Scheme 2).

- (ii) The TG and DTA curves of the Co and Ni complexes derived from adenine–salicylaldehyde (HL_4) pointed to that the dehydration of both complexes occurs in two successive steps at 328–460 and 430–510 K ranges corresponding to the removal of outer sphere and coordinated water molecules. The lower calculated E_a values suggest that the coordinated water molecule is more weakly bound in the nickel complex than in the corresponding cobalt. This is compatible with the difference in analytical data [17] of both complexes where only one outer sphere water molecule exists in case of Co^{II} complex, whereas in the Cu^{II} complex, two outer sphere water molecules are found [29]. Once dehydrated, the Co^{II} and Ni^{II} complexes are subjected to decomposition of nearly the same manner and ended with the formation of metal CoO and Ni metal, respectively [21] (Scheme 3).
- (iii) The change of entropy values, $\Delta S^\#$, for all complexes are nearly of the same magnitude and lie within the range -0.2344 to $-0.2592 \text{ kJ K}^{-1} \text{ mol}^{-1}$, all are with –ve signs. Therefore, the transition states are more ordered, i.e., in a less random molecular configuration than the reacting complexes. The fractions appeared in the calculated order of the

thermal reactions, n , Table 1, confirmed that the reactions proceeded in complicated mechanisms. Most of the peaks are of endo behavior and only three are of exo trend, $\text{Cu}\cdot 2\text{L}_1\cdot 2\text{Cl}$ (3rd peak), HL_4 (3rd peak) and HL_5 (very sharp peak) (Scheme 4).

- (iv) The calculated values of the collisions number, Z , showed a direct relation to E_a . The maximum and minimum Z values are 5.294 and 0.562, respectively, to suggest different mechanisms with variable speeds. The values of the decomposed substance fraction, α_m , at the maximum development of the reaction are of nearly the same magnitude and lie within the range 0.4473–0.7574. The maximum and the minimum T_m values are 940.05 and 328.38, respectively.

The plot of $\log(\alpha/T^2) + 10$ versus $1000/T$ from TG data gave straight lines intersect with each other at some phase transition temperatures (Table 2).

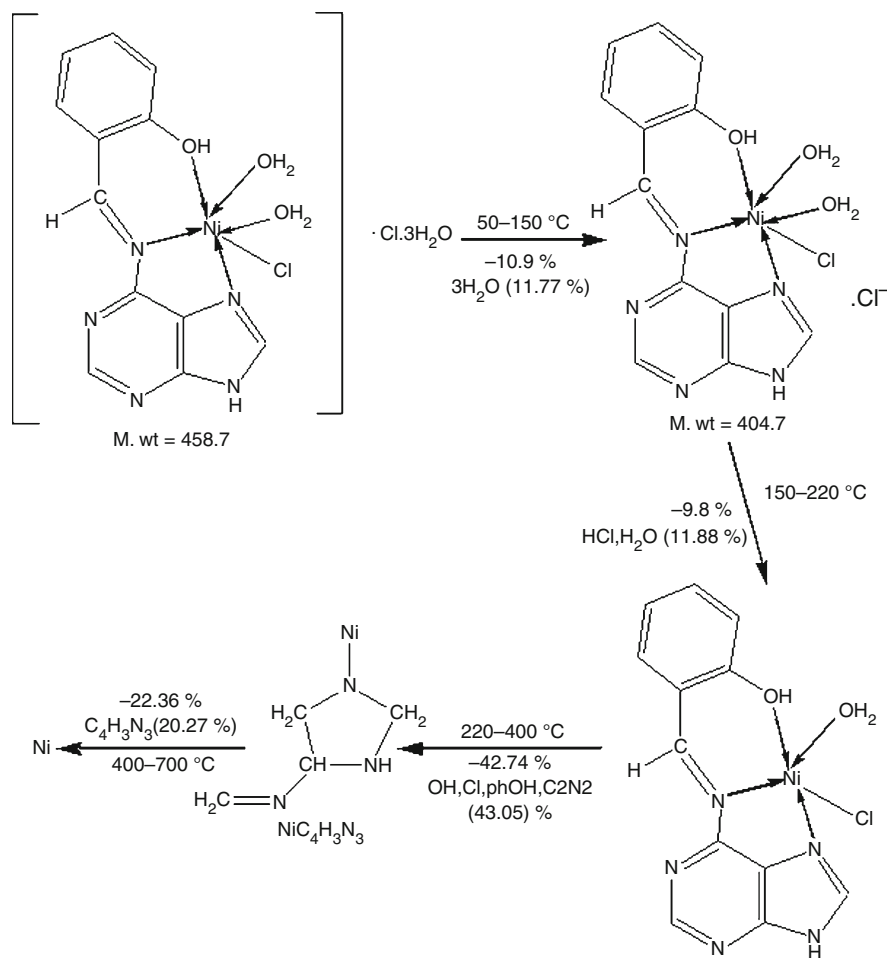
The TG data of adenine gave two well-characterized peaks, Fig. 1, in the temperature range 250–400 and 420–860 °C with a mechanism given as follows (Scheme 5).

The TG data of the Schiff base derived from adenine–salicylaldehyde compound gave three peaks lie in the temperature ranges: 75–200, 220–400, and 400–800 °C, respectively, Table 1. The mechanism of decomposition is illustrated as follows (Scheme 6).

Meanwhile the data of Schiff base adenine–acetylacetone gave well noticeable peak in the temperature range 140–420 °C, Fig. 1, and the following mode of decomposition is given (Scheme 7).

Similarly, TG curve of adenine azo resorcinol showed three peaks in the temperature ranges 140–240, 250–370,

Scheme 4 The TG mass losses of Ni-(HL₄)·2Cl·5H₂O complex



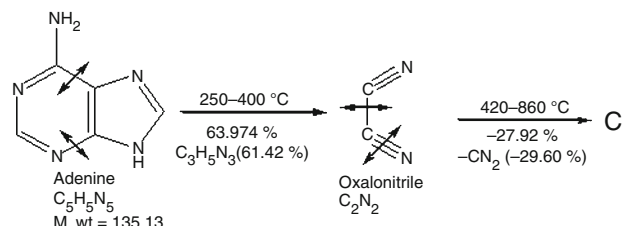
and 400–800 °C, Fig. 1, and the thermal pattern for decomposition can be outlined (Scheme 8).

The cadmium guanine complex gave two peaks at 50–350 and 360–500 °C of endo behavior, and the mechanism of decomposition is as follows (Scheme 9).

Table 2 Phase transition temperatures

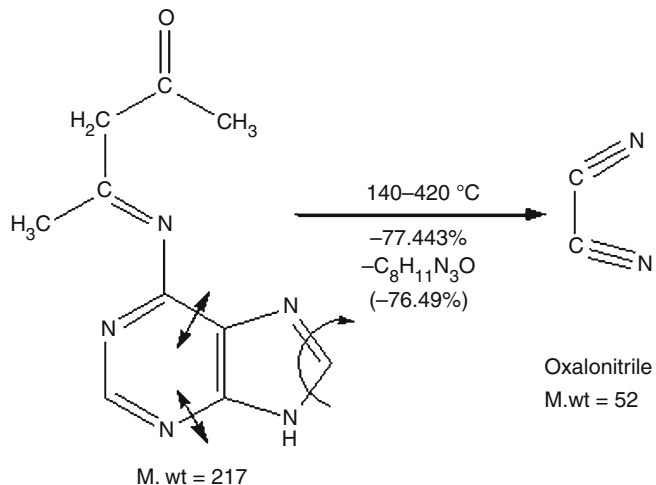
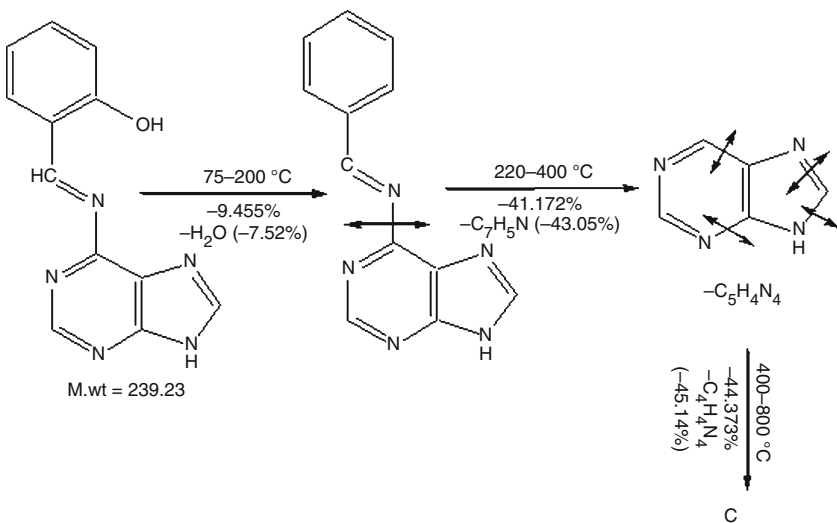
Compounds	Phase transition (K)
L ₁	653
HL ₃	623
HL ₄	591.75
HL ₅	598
Cu·2L ₁ ·2Cl	662.46
Co·(L ₁ -H)·2H ₂ O·Cl	403.4 and 523
Cd·L ₂ ·Cl·H ₂ O	407.31 and 573
Hg·(HL ₂)·2Cl·H ₂ O	523 and 673
Co·(HL ₃)·H ₂ O·2Cl	595.69
Co·(HL ₄)·4H ₂ O·2Cl	543.27
Ni·(HL ₄)·5H ₂ O·2Cl	385.53, 458.13, and 610.59

Also, the mercury guanine complex TG curve showed two endo peaks at 50–300 and 350–650 °C, Fig. 2. While cobalt adenine complex gave two peaks of endo behavior at 50–250 °C and 250–600 °C. However, the cobalt Schiff base adenine–acetylacetone complex gave three endo peaks at 50–250, 250–400, and 400–550 °C, where that of salicylaldehyde, Fig. 2, gave two endo peaks at 50–250 and 250–600 °C as follows (Scheme 10).



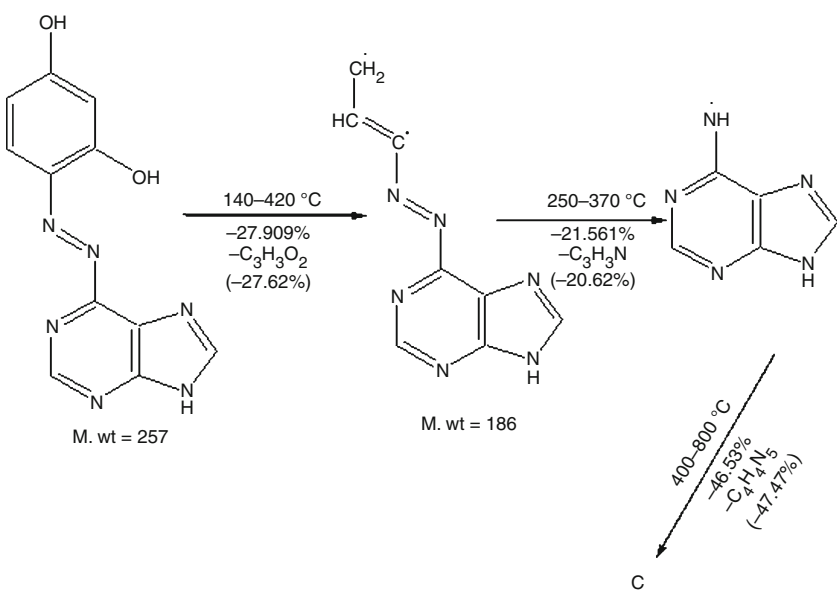
Scheme 5 The TG mass losses of adenine

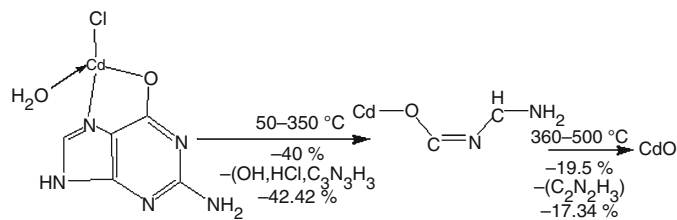
Scheme 6 The TG mass losses of the Schiff base derived from adenine-salicylaldehyde compound



Scheme 7 The TG mass losses of the Schiff base derived from adenine-acetylacetone

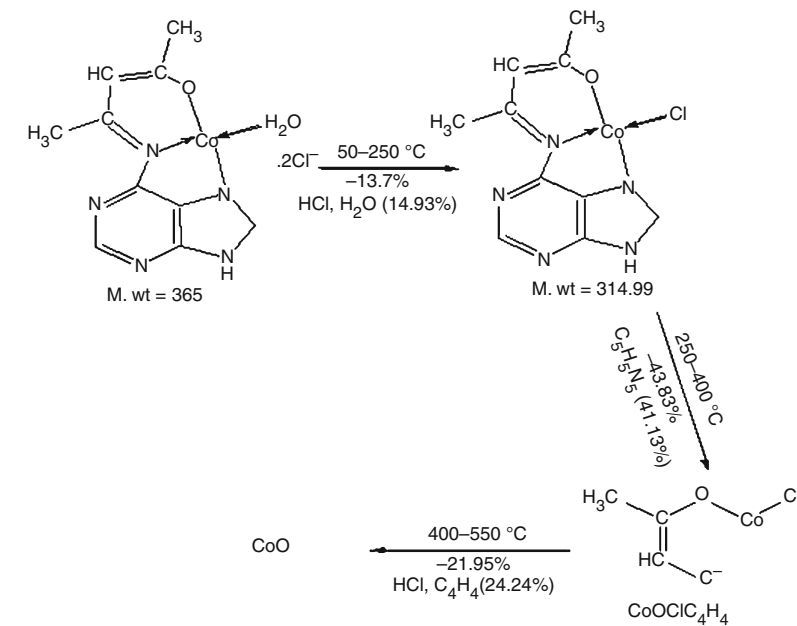
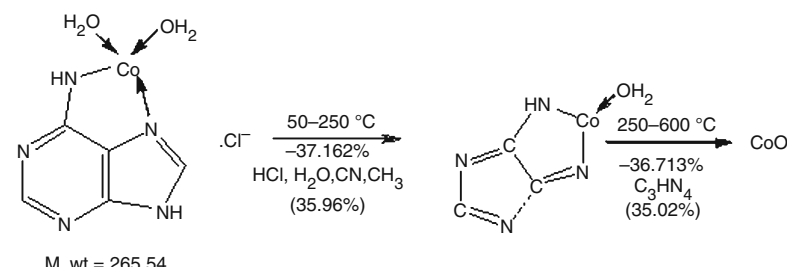
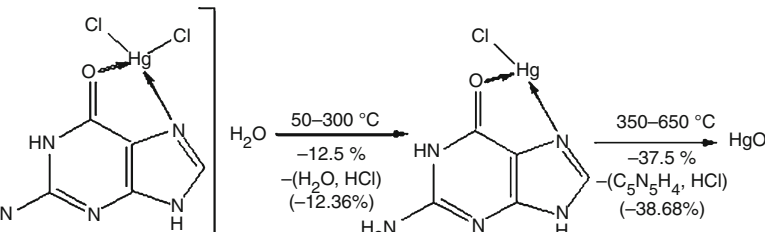
Scheme 8 The TG mass losses of adenine azo resorcinol





Scheme 9 The TG mass losses of cadmium guanine complex

Scheme 10 The TG mass losses of mercury guanine, cobalt adenine and cobalt Schiff base adenine-acetylacetone complexes



References

1. Chan HSO, Lusty JR. Thermal studies on some group VIII complexes with biologically active ligands. *J Therm Anal.* 1985;30:25–32.
2. Hueso F, Illán NA, Moreno MN, Martínez JM, Ramírez MJ. Synthesis and spectroscopic studies on the new Schiff base derived from the 1:2 condensation of 2,6-diformyl-4-methylphenol with 5-aminouracil (BDF5AU) and its transition metal complexes – Influence on biologically active peptides-regulating aminopeptidases. *J Inorg Biochem.* 2003;94:326–34.
3. Ibrahim DA, El-Metwally AM. Design, synthesis, and biological evaluation of novel pyrimidine derivatives as CDK2 inhibitors. *Eur J Med Chem.* 2010. doi: [10.1016/j.ejmech.2009.12.026](https://doi.org/10.1016/j.ejmech.2009.12.026).
4. Shapiro R. The prebiotic role of adenine: a critical analysis. *Origins Life Evol Biosphere.* 2005. doi: [10.1007/BF01581575](https://doi.org/10.1007/BF01581575).
5. Lippert B. Multiplicity of metal ion binding patterns to nucleobases. *Coord Chem Rev.* 2000;200:487–516.
6. Amo-Ochoa P, Sanz Miguel PJ, Castillo O, Sabat M, Lippert B, Zamora F. Interguanine hydrogen-bonding patterns in adducts with water and Zn-purine complexes (purine is 9-ethyladenine and 9-methylguanine). Unexpected preference of Zn(II) for adenine-N7 over guanine-N7. *J Biol Inorg Chem.* 2007;12:543–55.
7. Masoud MS, Ghonaim AKh, Ahmed RH, Abou El-Enein SA, Mahmoud AA. Ligating properties of 5-nitrobarbituric acid. *J Coord Chem.* 2002;55(1):79–105.
8. Masoud MS, Soayed AA, Ali AE, Sharsherh OK. Synthesis and characterization of new azopyrimidine complexes. *J Coord Chem.* 2003;56(8):725–42.
9. Masoud MS, Soayed AA, Ali AE. Complexing properties of nucleic-acid constituents adenine and guanine complexes. *Spectrochim Acta.* 2004;60A:1907–15.
10. Masoud MS, Kassem TS, Shaker MA, Ali AA. Studies on transition metal murexide complexes. *J Therm Anal Calorim.* 2006; 84:549–55.
11. Masoud MS, Haggag SS, Khalil EA. Complexing properties of some pyrimidines. *Nucleosides Nucleotides Nucleic Acids.* 2006; 25:73–87.
12. Masoud MS, Ibrahim AA, Khalil EA, El-Maghany AE. Spectral properties of some metal complexes derived from uracil-thiouracil and citrazinic acid compounds. *Spectrochim Acta.* 2007;67A: 662–8.
13. Masoud MS, Abou El-Enein SA, Ramadan AM, Goher AS. Thermal properties of some biologically active 5-(p-substituted phenylazo)-6-aminouracil complexes. *J Anal Appl Pyrolysis.* 2008;81:45–51.
14. Masoud MS, Amira MF, Ramadan AM, El-Ashry GM. Synthesis and characterization of some pyrimidine, purine, amino acid and mixed ligand complexes. *Spectrochim Acta.* 2008;69A:230–8.
15. Hammud HH, Bouhadir KH, Masoud MS, Ghannum AM, Assi SA. Solvent effect on the absorption and fluorescence emission spectra of some purine derivatives: spectrofluorometric quantitative studies. *J Solut Chem.* 2008;37:895–917.
16. Zawortko MJ, Hammud HH, Kabbani A, McManus GJ, Ghannoum AM, Masoud MS. Synthesis and characterization of some transition metal complexes with mixed adenine and acetylacetone ligands: crystal structures of solvated complex $\{[\text{Cu}(\text{acac})_2(\text{adenine})]\cdot\text{EtOH}\}$ and $\{[\text{Cu}(\text{acac})_2(\text{adenine})]\cdot\text{DMF}\cdot\text{H}_2\text{O}\}$. *J Chem Crystallogr.* 2009. doi: [10.1007/s10870-009-9575-3](https://doi.org/10.1007/s10870-009-9575-3).
17. Masoud MS, El-Merghany A, Abd El-Kawy MY. Synthesis and physico-chemical properties of biologically active purine complexes. *Synth React Inorg Met-Org Nano-Met Chem.* 2009;39(9): 537–53.
18. Soliman AA, Khattab MM, Linert W. Kinetic and characterization studies of iron(II) and iron(III) complex formation reactions with hydrazinopyridine. *J Coord Chem.* 2008;61:2017–31.
19. Omar MM. Spectral, thermal and biological activity studies on ruthenium(II) complexes with some pyridylamines. *J Therm Anal Calorim.* 2009;96:607–15.
20. Olar R, Badea M, Marinescu D, Lazar V, Chifiriac C. New complexes of Ni(II) and Cu(II) with Schiff bases functionalised with 1,3,4-thiadiazole: spectral, magnetic, biological and thermal characterisation. *J Therm Anal Calorim.* 2009;97:721–7.
21. Badea M, Olar R, Marinescu D, Lazar V, Chifiriac C, Vasile G. Thermal behaviour of new biological active cadmium mixed ligands complexes. *J Therm Anal Calorim.* 2009;97:781–5.
22. Kissinger E. Reaction kinetics in differential thermal analysis. *Anal Chem.* 1957;29:1702–06.
23. Oswald HR, Dubler E. In: Wiedemann HG, editors. *Thermal analysis*, vol. 2. Basel, Switzerland: Birkhäuser; 1972.
24. Horowitz H, Metzer G. A new analysis of thermogravimetric traces. *Anal Chem.* 1963;35:1464–68.
25. Dhar ML, Singh O. Kinetics and thermal decomposition of Fe(III) and UO₂(II) complexes with embelin (2,5-dihydroxy-3-undecyl-P-benzoquinone). *J Therm Anal.* 1991;37:259–65.
26. Traore K. Analyse thermique différentielle et cinétique de réaction III. Surface des pics d'analyse thermique différentielle et applications. *J Therm Anal.* 1972;4:135–45.
27. Piloyan GO, Ryabchikov ID, Novikova OS. Determination of activation energies of chemical reactions by differential thermal analysis. *Nature.* 1966;212:1229.
28. Moreno MN, Romero MA, Salas JM, Sánchez MP. Thermal analysis applied to the study of metal complexes: thermal behaviour of 6-amino-2-thiouracil and its complexes with several transition metal ions. *Thermochim Acta.* 1992;200:271–80.
29. Masoud MS, Khalil EA, Ramadan AM. Thermal properties of some Co^{II}, Ni^{II} and Cu^{II} complexes of new substituted pyrimidine compounds. *J Anal Appl Pyrolysis.* 2007;78:14–23.